

Synthesis of Azo-Conjugated Metalladithiolenes and Their Photo- and Proton-Responsive Isomerization Reactions

Masayuki Nihei,[†] Masato Kurihara, Jun Mizutani, and Hiroshi Nishihara*

Contribution from the Department of Chemistry, School of Science, The University of Tokyo, 7-3-1 Hongo, Bunkyo-ku, Tokyo 113-0033, Japan

Received August 9, 2002; E-mail: nisihara@chem.s.u-tokyo.ac.jp

Abstract: A versatile synthetic method of azo-conjugated metalladithiolenes was developed, and new complexes with various central metals and substituent groups were synthesized. Molecular structures of the azo-conjugated metalladithiolenes of Ni(II), Pd(II), and Pt(II) with diphenylphosphinoethane as a co-ligand were determined by X-ray crystallography. While the energy of the reversible trans-to-cis photoisomerization is considerably lower than that of azobenzene, the thermal stability of the cis form is much higher than that of the organic azobenzene derivatives showing similar low-energy trans-to-cis photoisomerization. A novel proton response of the azo group occurs, and the combination of photoisomerization and protonation leads to a novel proton-catalyzed cis-to-trans isomerization, the rate of which correlates with the redox potential of the metalladithiolene moiety. The study including other azo-conjugated metalladithiolenes has indicated that the protonation is a common feature for the azo-conjugated metalladithiolenes, but trans-to-cis photoisomerization is strongly dependent on the electronic structure of the trans form or a steric effect in the cis form.

Azobenzene¹ and its derivatives undergo reversible trans–cis isomerization in response to photo and thermal input, a mechanism to which much effort has been devoted.² Such isomerization of azobenzenes is the subject of current research interest in the area of photon-mode high-density information storage and photoswitching devices.³ Azo-conjugated transition metal complexes can provide new advanced molecular functions, based on combinations of photoisomerization of the azo group and changes in the intrinsic properties, that is, in the optical, redox, and magnetic properties, originating from the d-electrons. Some metal complexes including azobenzene and related compounds as a building block have already been synthesized,⁴ and a number of studies concerned with the photoisomerization of azo-conjugated metal complexes have appeared in recent

years.⁵ Some of them have shown novel behaviors which are not observed for organic azobenzenes, such as redox-combined single light reversible isomerization,^{6d,h} MLCT photoisomerization,^{6f,h} and isomerization-promoted photoluminescence switching,^{5a,c} indicating that the type of attached metal complexes controls such functionalities.

Metalladithiolene,⁷ which is known to exhibit a noninnocent character originating from its quasi-aromaticity and a strong π -electron donor ability due to the involvement of sulfur atoms, is one of the representative transition metal complexes of present interest. These complexes have attracted attention as components in magnetic⁸ and conducting materials,⁹ as models for the molybdenum cofactor (Moco),¹⁰ and as solution lumiphore.¹¹

[†] Present address: Department of Chemistry, University of Tsukuba, Tennodai 1-1-1, Tsukuba, Ibaraki 305-8571, Japan. E-mail: nihei@staff.chem.tsukuba.ac.jp.

* To whom correspondence should be addressed. Fax: +81-3-5841-8063. Tel: +81-3-5841-4346.

- (1) (a) Rau, H. *Photochromic Molecules and Systems*; Elsevier: Amsterdam, 1990; Chapter 4. (b) Anzai, J.; Osa, T. *Tetrahedron* **1994**, *50*, 4039. (c) Rau, H. *Angew. Chem., Int. Ed. Engl.* **1973**, *12*, 224.
- (2) (a) Dürr, H., Laurent, H. B., Eds. *Photochromism: Molecules and Systems*; Elsevier: Amsterdam, 1990. (b) Tamai, N.; Miyasaka, H. *Chem. Rev.* **2000**, *100*, 1875 and references therein. (c) Kojima, M.; Takagi, T.; Karatsu, T. *Chem. Lett.* **2000**, 686.
- (3) (a) Liu, Z. F.; Hashimoto, K.; Fujishima, A. *Nature* **1990**, *347*, 658. (b) Ikeda, T.; Tsutsumi, O. *Science* **1995**, *268*, 1873. (c) Kawata, S.; Kawata, Y. *Chem. Rev.* **2000**, *100*, 1777. (d) Ichimura, K. *Chem. Rev.* **2000**, *100*, 1847.
- (4) (a) Das, A.; Maher, J. P.; McCleverty, J. A.; Badiola, J. A. N.; Ward, M. D. *J. Chem. Soc., Dalton Trans.* **1993**, 681. (b) Otsuki, J.; Tsujino, M.; Iizaki, T.; Araki, K.; Seno, M.; Takatera, K.; Watanabe, T. *J. Am. Chem. Soc.* **1997**, *119*, 7895. (c) Noro, S.; Kondo, M.; Ishii, T.; Kitagawa, S.; Matsuzaka, H. *J. Chem. Soc., Dalton Trans.* **1999**, 1569. (d) Sun, S. S.; Lees, A. J. *J. Am. Chem. Soc.* **2000**, *122*, 8956. (e) Mosher, P. J.; Yap, G. P. A.; Crutchley, R. J. *Inorg. Chem.* **2001**, *40*, 1189. (f) Li, B.; Liu, H.; Xu, Y.; Yin, G.; Chen, J.; Xu, Z. *Chem. Lett.* **2001**, 214.
- (5) (a) Yam, V. W. W.; Lau, V. C. Y.; Wu, L. X. *J. Chem. Soc., Dalton Trans.* **1998**, 1461. (b) Hayami, S.; Inoue, K.; Osaki, S.; Maeda, Y. *Chem. Lett.* **1998**, 987. (c) Tsuchiya, S. *J. Am. Chem. Soc.* **1999**, *121*, 48. (d) Otsuki, J.; Harada, K.; Araki, K. *Chem. Lett.* **1999**, 269. (e) Aiello, I.; Ghedini, M.; Deda, M. L.; Pucci, D.; Francescangeli, O. *Eur. J. Inorg. Chem.* **1999**, 1367. (f) Barigelletti, F.; Ghedini, M.; Pucci, D.; Deda, M. L. *Chem. Lett.* **1999**, 297. (g) Miyaki, Y.; Onishi, T.; Kurosawa, H. *Chem. Lett.* **2000**, 1334.
- (6) (a) Yutaka, T.; Kurihara, M.; Nishihara, H. *Mol. Cryst. Liq. Cryst.* **2000**, *343*, 193. (b) Yutaka, T.; Kurihara, M.; Kubo, K.; Nishihara, H. *Inorg. Chem.* **2000**, *39*, 3438. (c) Yutaka, T.; Mori, I.; Kurihara, M.; Mizutani, J.; Kubo, K.; Furusho, S.; Matsumura, K.; Tamai, N.; Nishihara, H. *Inorg. Chem.* **2001**, *40*, 4986. (d) Kume, S.; Kurihara, M.; Nishihara, H. *Chem. Commun.* **2001**, 1656. (e) Kurosawa, M.; Nankawa, T.; Matsuda, T.; Kubo, K.; Kurihara, M.; Nishihara, H. *Inorg. Chem.* **1999**, *38*, 5113. (f) Kurihara, M.; Matsuda, T.; Hirooka, A.; Yutaka, T.; Nishihara, H. *J. Am. Chem. Soc.* **2000**, *122*, 12373. (g) Kurihara, M.; Nishihara, H. *Coord. Chem. Rev.* **2002**, *226*, 125. (h) Kurihara, M.; Hirooka, A.; Kume, S.; Sugimoto, M.; Nishihara, H. *J. Am. Chem. Soc.* **2002**, *124*, 8800.
- (7) (a) McCleverty, J. A. *Prog. Inorg. Chem.* **1969**, *2*, 72. (b) Burns, R. P.; McAullife, C. A. *Adv. Inorg. Chem. Radiochem.* **1979**, *22*, 303. (c) Müller-westerhoff, U. T. In *Comprehensive Coordination Chemistry*; Vance, B., Wilkinson, G., Gillard, R. D., McCleverty, J. A., Eds.; Pergamon: Oxford, 1987; Vol. 2, pp 595–631. (d) Fourmigue, M. *Coord. Chem. Rev.* **1998**, *178–180*, 823. (e) Sugimori, A.; Akiyama, T.; Kajitani, M.; Sugiyama, T. *Bull. Chem. Soc. Jpn.* **1999**, *72*, 879.

Metalladithiolenes possess a highly delocalized bonding description.⁷ Moreover, strong electronic interactions between metalladithiolenes and the azo group can be anticipated by the conjugation of the metalladithiolenes and the azo group, which introduces the potential for novel functionality of the azobenzene moiety.

In a previous communication, we reported preliminary results concerning the synthesis of azo-conjugated platinadithiolenes and its photo and proton response and novel proton-coupled cis-to-trans isomerization originating from the strong electronic interactions between the metalladithiolenes and the azo moieties.¹² Although the protonated product of azobenzene derivatives has been recognized for a long time,¹³ reports on proton-catalyzed isomerization of azobenzene derivatives have not been available to our knowledge. In this paper, we report the development of a novel versatile method of synthesizing azo-conjugated metalladithiolenes systems, and also the curious proton response and proton-catalyzed cis-to-trans isomerization for dppe-M (M = Ni, Pd, and Pt) complexes. This study provides a systematic investigation of the dependence of the types of central metal and substituents on isomerization in the azo moiety.

Experimental Section

Materials. 5-Nitro-2-thioxo-1,3-benzenedithiol, [1,2-bis(diphenylphosphino)ethane]dichloroplatinum(II), [1,2-bis(diphenylphosphino)ethane]dichloropalladium(II), and CpCo(III)I₂(CO) (Cp = η⁵-cyclopentadienyl) were prepared according to the literature.¹⁴ Zinc powder, iron(III) trichloride, and nickel(II) trichloride were purchased from Wako Chemicals, and all other materials and solvents were purchased from Kanto Chemicals. Anhydrous solvents were used after distillation from CaH₂. Tetrahydrofuran was purchased from Kanto Chemicals and was used after drying by passage through a molecular sieve column and degassing. Spectroscopic-grade solvents (Kanto Chemicals) were used for UV-vis absorption spectroscopy. The solvents for electrochemical measurement were of HPLC grade (Kanto Chemicals). For the electrochemical measurements, tetrabutylammonium perchlorate was purchased from Tomiyama Chemicals and was used after recrystallization from methanol.

Apparatus. UV-vis, IR, and ¹H NMR spectra were recorded with Jasco V-570 and Hewlett-Packard 8453 UV-vis spectrometers, a Jasco FT/IR-620v spectrometer, and a JEOL EX270 spectrometer, respectively. Photoisomerization measurements were carried out under a nitrogen atmosphere using a USHIO 500W super high-pressure USH-500D mercury lamp as an irradiation source. The monochromatic light was obtained with a Jasco CT-10T monochromator.

Electron Spray Ionization (ESI) Mass Spectrometry Measurements. ESI mass spectra (ESI MS) were obtained with a Micromass LCT time-of-flight mass spectrometer. Each sample was infused as an acetonitrile solution. Cone voltage was varied in the range from 30 to 60 V to obtain clear peaks.

Electrochemical Measurements. A glassy carbon rod (diameter 5 mm; Tokai Carbon GC-20) was embedded in Pyrex glass, and the cross section was used as a working electrode. Cyclic voltammetry measurements were carried out in a standard one-compartment cell under Ar equipped with a platinum-wire counter electrode and an Ag/Ag⁺ reference electrode (10 mM AgClO₄ in 0.1 M Bu₄NClO₄-MeCN, E⁰-(ferrocene/ferrocene) (Fc^{+/0}/Fc) in 0.1 M Bu₄NClO₄/CH₂Cl₂) = 0.077 V vs Ag/Ag⁺) with a BAS CV-50W voltammetric analyzer.

Determination of Cis-to-Trans Thermal Isomerization Rate Constants. A 1-cm light path-length quartz cell was used for the photoisomerization measurements. The sample solution was degassed by N₂ bubbling before photoirradiation. The time course change in absorbance was measured by a Hewlett-Packard 8453 UV-vis spectrometer, and the temperature was controlled by a Hewlett-Packard 89090A Peltier Temperature Control Accessory. The cis-to-trans thermal isomerization obeyed first-order kinetics, with the isomerization rate constant, *k*, being evaluated from the change in absorbance by the following equation:

$$\ln\{(A_0 - A_\infty)/(A_t - A_\infty)\} = kt \quad (1)$$

where *A*₀, *A*_∞, and *A*_{*t*} denote the absorbance at time *t* = 0, *t*, and ∞, respectively. Both *k* and *A*_∞ were evaluated by a nonlinear least-squares calculation.

X-ray Crystallography. Crystals of **12–14** obtained by recrystallization from dichloromethane/hexane were mounted on a glass loop, and data were collected at 173 K (Rigaku Mercury diffractometer coupled with a CCD area detector with graphite monochromated Mo Kα radiation (0.7107 Å)). An empirical absorption correction was applied, that resulted in transmission factors ranging from 0.74 to 1.03 for **13** and from 0.44 to 1.04 for **14**, respectively. The structure was solved by direct methods and expanded using Fourier techniques. Hydrogen atoms were not included in the calculations. The final cycle of full-matrix least-squares refinement on *F* was based on 6563 observed reflections (*I* > -10.0σ(*I*)) for **12**, on 8870 observed reflections (*I* > 1.50σ(*I*)) for **13**, and on 3990 observed reflections (*I* > 3.00σ(*I*)) for **14**. All calculations were performed using the CrystalStructure crystallographic software package of the Rigaku Corp. and the Molecular Structure Corp. (the crystallographic data are given in Table S1, Supporting Information).

Synthesis. 5-Nitroso-1,3-benzodithiole-2-thione, 2. Zinc powder was slowly added to a mixture of **1** (1.00 g, 4.37 mmol) in 2-methoxyethanol (120 mL) and ammonium chloride (350 mg, 6.56 mmol) in water (10 mL) over a 30 min period. After the mixture was stirred for an additional 1 h, the residue was filtered. The filtrate was added dropwise over a period of 1 h to a stirred solution of 2.84 g (10.5 mmol) of FeCl₃·6H₂O in ethanol (24 mL) and water (96 mL) at -15 °C, and then it was filtered and washed with water. The residue was dried to yield 691 mg (3.24 mmol, 74.2%) of **2**. Anal. Calcd for C₇H₃N₁O₁S₃·0.6H₂O: C, 37.52; H, 1.89; N, 6.25. Found: C, 37.43; H, 1.95; N, 5.99. ¹H NMR (270 MHz, CDCl₃, 25 °C): δ 8.03 (dd, *J* = 8.1, 1.6 Hz, 1H, Ph), 7.87 (d, *J* = 1.6 Hz, 1H, Ph), 7.73 (d, *J* = 8.1 Hz, 1H, Ph).

5-Amino-1,3-benzodithiole-2-thione, 3. An ethanol solution of SnCl₂·6H₂O (5.91 g, 26.19 mmol) was added to a stirred solution of **1** (2.00 g, 8.73 mmol) in hydrochloric acid (90 mL) and ethanol (45 mL), and then refluxed for 13 h. The slurry was filtered, and the solid was dissolved with ethyl acetate and washed three times with aqueous NaHCO₃. The organic solution was then evaporated and purified by silica gel column chromatography with chloroform as an eluent. The product was recrystallized from dichloromethane/methanol to yield

- (8) (a) Manoharan, P. T.; Noordik, J. H.; de Boer, E.; Keijzers, C. P. *J. Chem. Phys.* **1981**, *74*, 1980. (b) Kuppusamy, P.; Manoharan, P. T. *Chem. Phys. Lett.* **1985**, *118*, 159.
- (9) (a) Cassoux, P.; Valade, L.; Kobayashi, H.; Kobayashi, A.; Clark, R. A.; Underhill, A. E. *Coord. Chem. Rev.* **1991**, *110*, 115. (b) Oik, R. M.; Oik, B.; Dietzch, W.; Kirmse, R.; Hoyer, E. *Coord. Chem. Rev.* **1992**, *117*, 99. (c) Fourmigue, M.; Lenoir, C.; Guyon, F.; Amaudrut, J. *Inorg. Chem.* **1995**, *34*, 4979.
- (10) (a) Hille, R. *Chem. Rev.* **1996**, *96*, 2757. (b) Hsu, J. K.; Bonangelino, C. J.; Kaiwer, S. P.; Boggs, C. M.; Fettingner, J. C.; Pilato, R. S. *Inorg. Chem.* **1996**, *35*, 4743.
- (11) (a) Zuleta, J. A.; Burberry, M. S.; Eisenberg, R. *Coord. Chem. Rev.* **1990**, *97*, 47. (b) Cummings, D. S.; Eisenberg, R. *Inorg. Chem.* **1995**, *34*, 2007. (c) Bevilacqua, M. J.; Eisenberg, R. *Inorg. Chem.* **1994**, *33*, 2913. (d) Cummings, D. S.; Eisenberg, R. *J. Am. Chem. Soc.* **1996**, *118*, 1949. (e) Kaiwer, S. P.; Vodacek, A.; Blouff, N. V.; Pilato, R. S. *J. Am. Chem. Soc.* **1997**, *119*, 3311.
- (12) Nihei, M.; Kurihara, M.; Mizutani, J.; Nishihara, H. *Chem. Lett.* **2001**, 852.
- (13) Hewitt, J. T.; Pope, F. G. *Chem. Ber.* **1897**, *30*, 1624.
- (14) (a) Nakayama, J.; Sugiura, H.; Hoshino, M. *Tetrahedron Lett.* **1983**, *24*, 2585. (b) McDermott, J. X.; White, J. F.; Whitesides, G. M. *J. Am. Chem. Soc.* **1976**, *98*, 6521. (c) Ozawa, F. In *Synthesis of Organometallic Compounds*; Komiya, S., Ed.; Wiley: New York, 1997; p 285. (d) King, R. B. *Inorg. Chem.* **1966**, *5*, 82.

0.794 g (3.99 mmol, 45.7%) of **3**. Anal. Calcd for $C_7H_5N_1S_3$: C, 42.18; H, 2.53; N, 7.03. Found: C, 42.41; H, 2.63; N, 7.08. 1H NMR (270 MHz, $CDCl_3$, 25 °C): δ 7.22 (d, $J = 8.6$ Hz, 1H, Ph), 6.77 (d, $J = 1.9$ Hz, 1H, Ph), 6.72 (dd, $J = 8.6$, 1.9 Hz, 1H, Ph), 3.88 (s, 2H, NH_2).

5-(Phenylazo)-1,3-benzodithiole-2-thione, 4. A mixture of **2** (450 mg, 2.11 mmol) and aniline (192 μ L, 2.11 mmol) in methanol (125 mL) and acetic acid (25 mL) was refluxed for 21 h. The solution was concentrated to 40 mL and cooled to 4 °C, and the precipitate was then filtered and washed with methanol. The resulting crude product was purified by silica gel column chromatography with chloroform/hexane (1/1, v/v) as an eluent. Recrystallization from methanol afforded 111 mg (0.386 mmol, 19.5%) of **4**. Anal. Calcd for $C_{13}H_7N_2S_3Cl$: C, 54.14; H, 2.80; N, 9.71. Found: C, 53.96; H, 2.89; N, 9.69. 1H NMR (270 MHz, $CDCl_3$, 25 °C): δ 8.03 (d, $J = 2.2$ Hz, 1H, Ph), 8.00 (dd, $J = 8.4$, 2.2 Hz, 1H, Ph), 7.96–7.91 (m, 2H, Ph), 7.62 (d, $J = 8.4$ Hz, 1H, Ph), 7.59–7.49 (m, 3H, Ph).

5-[(4-Methylphenyl)azo]-1,3-benzodithiole-2-thione, 5. **5** was synthesized in the same manner as **4**. Yield: 43.0%. Anal. Calcd for $C_{14}H_{10}N_2S_3 \cdot 0.25H_2O$: C, 54.78; H, 3.45; N, 9.13. Found: C, 54.86; H, 3.32; N, 9.19. 1H NMR (270 MHz, $CDCl_3$, 25 °C): δ 8.01 (d, $J = 1.6$ Hz, 1H, Ph), 7.97 (dd, $J = 8.4$, 1.6 Hz, 1H, Ph), 7.84 (d, $J = 8.1$ Hz, 2H, Tol), 7.61 (d, $J = 8.4$ Hz, 1H, Ph), 7.34 (d, $J = 8.1$ Hz, 2H, Tol), 2.46 (s, 3H, Me).

5-[(4-Chlorophenyl)azo]-1,3-benzodithiole-2-thione, 6. **6** was synthesized in the same manner as **4**. Yield: 19.5%. Anal. Calcd for $C_{13}H_7N_2S_3Cl$: C, 48.36; H, 2.19; N, 8.68. Found: C, 48.14; H, 2.28; N, 8.71. 1H NMR (270 MHz, $CDCl_3$, 25 °C): δ 8.02 (d, $J = 1.4$ Hz, 1H, Ph), 7.98 (dd, $J = 8.4$, 1.4 Hz, 1H, Ph), 7.89 (d, $J = 8.4$ Hz, 2H, Ph), 7.62 (d, $J = 8.4$ Hz, 1H, Ph), 7.51 (d, $J = 8.4$ Hz, 2H, Ph).

5-[(4-Methoxyphenyl)azo]-1,3-benzodithiole-2-thione, 7. **7** was synthesized in the same manner as **4**. Yield: 35.0%. Anal. Calcd for $C_{14}H_{10}ON_2S_3$: C, 52.80; H, 3.17; N, 8.80. Found: C, 52.55; H, 3.19; N, 8.80. 1H NMR (270 MHz, $CDCl_3$, 25 °C): δ 7.97 (d, $J = 1.9$ Hz, 1H, Ph), 7.95 (dd, $J = 8.1$, 1.9 Hz, 1H, Ph), 7.93 (d, $J = 9.5$ Hz, 2H, Ph), 7.59 (d, $J = 8.1$ Hz, 1H, Ph), 7.03 (d, $J = 9.5$ Hz, 2H, Ph), 3.91 (s, 3H, OMe).

5,5'-Azobis(1,3-benzodithiole-2-thione), 8. A mixture of **2** (326 mg, 1.53 mmol) and **3** (350 mg, 1.53 mmol) in chloroform (200 mL), methanol (70 mL), and acetic acid (70 mL) was refluxed for 3 days. The clear solution was then turned to slurry, and the orange precipitate was collected and washed with methanol to yield 296 mg of **8** (0.75 mmol, 49.0%). Anal. Calcd for $C_{14}H_6N_2S_6$: C, 42.61; H, 1.53; N, 7.10. Found: C, 42.36; H, 1.67; N, 6.94. 1H NMR (270 MHz, $CDCl_3$, 25 °C): δ 8.04 (d, $J = 1.9$ Hz, 1H, Ph), 8.00 (dd, $J = 8.7$, 1.9 Hz, 1H, Ph), 7.64 (d, $J = 8.7$ Hz, 2H, Ph).

All manipulations described below were carried out under a nitrogen atmosphere.

1,2-Bis(diphenylphosphino- κP)ethane[4-(phenylazo)-1,2-benzenedithiolato- $\kappa S, \kappa S'$]nickel(II), 9. Phenyllithium (0.38 mL, 0.40 mmol) was added dropwise to a stirred solution of **4** (58 mg, 0.20 mmol) in THF (25 mL) maintained at –15 °C, and the resulting solution was then stirred for 10 h, while the temperature was allowed to increase to room temperature. $dppeNiCl_2$ powder (105 mg, 0.20 mmol) was then added to the solution, which was stirred further for 2 h. The resulting mixture was separated by silica gel column chromatography using dichloromethane/hexane (1/1, v/v) as an eluent. The yellow-band component was collected, and the solvent was evaporated. Recrystallization from dichloromethane/hexane yielded 25.6 mg (0.026 mmol, 18.2%) of **9** as a red powder. Anal. Calcd for $C_{38}H_{32}N_2P_2S_2Ni$: C, 65.07; H, 4.60; N, 3.99. Found: C, 64.85; H, 4.53; N, 4.01. 1H NMR (270 MHz, $CDCl_3$, 25 °C): δ 8.00 (s, 1H, Ph), 7.86–7.79 (m, 10H, dppe, Ph), 7.54–7.27 (m, 16H, dppe, Ph), 7.31 (d, $J = 8.4$ Hz, 1H, Ph), 2.40 (d, $J_{PH} = 17.6$ Hz, 4H, dppe).

[1,2-Bis(diphenylphosphino- κP)ethane][4-[(4-chlorophenyl)azo]-1,2-benzenedithiolato- $\kappa S, \kappa S'$]nickel(II), 10. **10** was synthesized in the same manner as **9**. Yield: 23.3%. Anal. Calcd for $C_{38}H_{31}N_2P_2S_2-$

$CINi$: C, 62.02; H, 4.25; N, 3.81. Found: C, 61.99; H, 4.30; N, 3.84. 1H NMR (270 MHz, $CDCl_3$, 25 °C): δ 7.99 (s, 1H, Ph), 7.86–7.80 (m, 8H, dppe), 7.76 (d, $J = 8.6$ Hz, 2H, Ph), 7.52–7.45 (m, 14H, dppe, Ph), 7.39 (d, $J = 8.6$ Hz, 2H, Ph), 2.40 (d, $J_{PH} = 17.8$ Hz, 4H, dppe).

[1,2-Bis(diphenylphosphino- κP)ethane][4-[(4-methoxyphenyl)azo]-1,2-benzenedithiolato- $\kappa S, \kappa S'$]nickel(II), 11. **11** was synthesized in the same manner as **9**. Yield: 19.0%. Anal. Calcd for $C_{39}H_{34}ON_2P_2S_2-Ni \cdot 0.5H_2O$: C, 63.26; H, 4.76; N, 3.78. Found: C, 63.56; H, 4.53; N, 3.84. 1H NMR (270 MHz, $CDCl_3$, 25 °C): δ 7.97 (s, 1H, Ph), 7.87–7.79 (m, 10H, dppe, Ph), 7.53–7.44 (m, 14H, dppe, Ph), 6.95 (d, $J = 9.2$ Hz, 2H, Ph), 3.85 (s, 3H, OMe), 2.40 (d, $J_{PH} = 17.8$ Hz, 4H, dppe).

[1,2-Bis(diphenylphosphino- κP)ethane][4-[(4-methylphenyl)azo]-1,2-benzenedithiolato- $\kappa S, \kappa S'$]nickel(II), 12. **12** was synthesized in the same manner as **9**. Yield: 13.1%. Anal. Calcd for $C_{39}H_{34}N_2P_2S_2-Ni \cdot 2H_2O$: C, 62.33; H, 5.10; N, 3.73. Found: C, 62.30; H, 5.09; N, 3.81. 1H NMR (270 MHz, $CDCl_3$, 25 °C): δ 7.98 (s, 1H, Ph), 7.86–7.80 (m, 8H, dppe), 7.53–7.45 (m, 14H, dppe, Ph), 7.71 (d, $J = 8.4$ Hz, 2H, Tol), 7.23 (d, $J = 8.4$ Hz, 2H, Tol), 2.39 (d, $J_{PH} = 17.6$ Hz, 4H, dppe), 2.38 (s, 3H, Me).

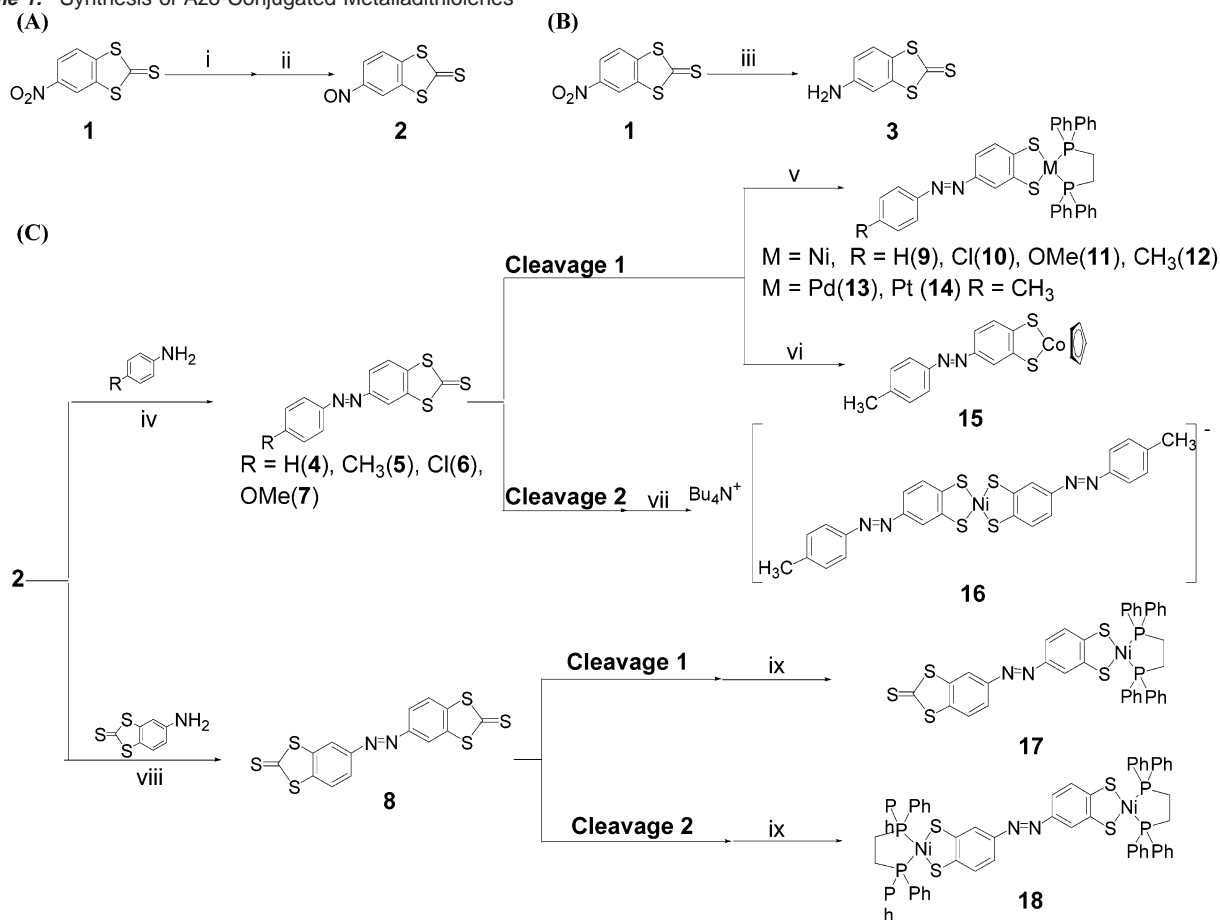
[1,2-Bis(diphenylphosphino- κP)ethane][4-[(4-methylphenyl)azo]-1,2-benzenedithiolato- $\kappa S, \kappa S'$]palladium(II), 13. Phenyllithium (0.38 mL, 0.40 mmol) was added dropwise to a stirred solution of **5** (60 mg, 0.20 mmol) in THF (25 mL) at –15 °C and stirred for 10 h, allowing the temperature to increase to room temperature. $dppePdCl_2$ powder (115 mg, 0.20 mmol) was then added to the solution, which was stirred further for 2 h. The resulting mixture was separated by silica gel column chromatography using dichloromethane/hexane (1/1, v/v) as an eluent. The yellow-band component was collected, and the solvent was evaporated. Recrystallization from dichloromethane/hexane yielded 7.9 mg (0.010 mmol, 5.2%) of **13** as fine yellow crystals. Anal. Calcd for $C_{39}H_{34}N_2P_2S_2Pd$: C, 61.38; H, 4.49; N, 3.67. Found: C, 61.25; H, 4.66; N, 3.72. 1H NMR (270 MHz, $CDCl_3$, 25 °C): δ 7.98 (d, $J = 2.2$ Hz, 1H, Ph), 7.89–7.79 (m, 8H, dppe), 7.72 (d, $J = 8.1$ Hz, 2H, Tol), 7.54–7.26 (m, 14H, dppe), 7.24 (d, $J = 8.1$ Hz, 2H, Tol), 2.54 (d, $J_{PH} = 20.1$ Hz, 4H, dppe), 2.38 (s, 3H, Me).

[1,2-Bis(diphenylphosphino- κP)ethane][4-[(4-methylphenyl)azo]-1,2-benzenedithiolato- $\kappa S, \kappa S'$]platinum(II), 14. Phenyllithium (0.38 mL, 0.40 mmol) was added dropwise to a stirred solution of **5** (60 mg, 0.20 mmol) in THF (25 mL) at –15 °C and was stirred for 10 h, allowing the temperature to increase to room temperature. $dppePtCl_2$ powder (133 mg, 0.20 mmol) was then added to the solution, which was stirred further for 2 h. The resulting mixture was separated by silica gel column chromatography using dichloromethane/hexane (1/1, v/v) as an eluent. The yellow-band component was collected, and the solvent was evaporated. Recrystallization from dichloromethane/hexane yielded 14.0 mg (0.016 mmol, 8.2%) of **14** as fine yellow crystals. Anal. Calcd for $C_{39}H_{34}N_2P_2S_2Pt$: C, 54.99; H, 4.02; N, 3.29. Found: C, 54.90; H, 4.08; N, 3.30. 1H NMR (270 MHz, $CDCl_3$, 25 °C): δ 8.12 (d, $J = 2.2$ Hz, 1H, Ph), 7.92–7.78 (m, 8H, dppe), 7.74 (d, $J = 8.4$ Hz, 2H, Tol), 7.50–7.47 (m, 12H, dppe), 7.62 (d, $J = 8.1$ Hz, 1H, Ph), 7.43 (dd, $J = 2.2$, 8.1 Hz, 1H, Ph), 7.24 (d, $J = 8.4$ Hz, 2H, Tol), 2.51 (d, $J_{PH} = 18.1$ Hz, 4H, dppe), 2.39 (s, 3H, Me).

Results and Discussion

Synthesis of Azo-Conjugated Metalladithiolenes. Several synthetic methods of metalladithiolenes have been previously reported. The methods used for the synthesis of metallo-1,2-ethylenedithiolates have been well established,^{7,15} but the

- (15) Wang, K.; McConnachie, J. M.; Stiefel, E. I. *Inorg. Chem.* **1999**, *38*, 4334. (b) Kaiwer, S. P.; Hsu, J. K.; Vodacek, A.; Yap, G.; Liabe-Sands, L. M.; Rheingold, A. L.; Pilato, R. S. *Inorg. Chem.* **1997**, *36*, 2406. (c) Davies, E. S.; Beddoes, R. L.; Collison, D.; Dinsmore, A.; Docrat, A.; Joule, J. A.; Wilson, C. R.; Garner, C. D. *J. Chem. Soc., Dalton Trans.* **1997**, 3985. (d) Hsu, J. K.; Bonangelino, C. J.; Kaiwar, S. P.; Boggs, C. M.; Fetting, J. C.; Pilato, R. S. *Inorg. Chem.* **1996**, *35*, 4743. (e) Nakayama, J.; Choi, K. S.; Akiyama, I.; Hoshino, M. *Tetrahedron Lett.* **1993**, *34*, 115.

Scheme 1. Synthesis of Azo-Conjugated Metalladithiolenes^a

^a Reagents: (i) Zn, NH₄Cl, MeOCH₂CH₂OH; (ii) FeCl₃·6H₂O; (iii) SnCl₂·6H₂O, HCl; (iv) CH₃COOH, MeOH; (v) MCl₂(dppe); (vi) CpCoI₂(CO); (vii) NiCl₂·6H₂O, Bu₄NBr; (viii) CH₃COOH, MeOH, CHCl₃; (ix) NiCl₂.

methods for synthesizing metallo-1,2-benzenedithiolates remain few in number.¹⁶ The most versatile and general method of preparing metallo-benzenedithiolenes is a reaction involving a benzenedithiolate dianion and a metal halide.^{16a} Benzenedithiolate is highly sensitive to oxidation¹⁷ and is unstable in air. Thus, the key elements in the synthetic strategy of the azo-conjugated metalladithiolene system are (1) how to protect the dithiolate group from reduction and oxidation while constructing the azo group, and (2) how to create the metalladithiolene component after a cleavage of the protecting group. To address these issues, we developed a versatile method of synthesizing azo-conjugated metalladithiolenes, as described in Scheme 1.

Nitroso compound **2** derived from nitro compound **1** is a novel dithiolate-protected compound, which can react with a number of organic and other functional molecules containing amino groups to afford various asymmetric and symmetric azo-conjugated metalladithiolenes. This protecting group can be cleaved by either basic media or nucleophilic reagents, whereas it is stable in strong acidic media and is resistant to strong reduction and mild oxidation. Thus, this group is one of the most suitable protecting groups for the construction of the azo group by reduction and oxidation in acidic media. The versatility of this synthetic method was demonstrated by the preparation

of the precursors, **4–8**, from compound **2** and the corresponding anilines. Reactions of **2** and aniline derivatives in mild acidic media afforded precursors of metalladithiolene ligands with various substituent groups, **4–7**, in moderate yields (Scheme 1C). The precursor of azo-bridged dinuclear metalladithiolene ligand **8** was prepared by the reaction of **2** and amino compound **3**, obtained by the reduction of nitro compound **1** with tin(II) chloride in hydrochloric acid in a moderate yield (Scheme 1B). This condensation reaction can be carried out under gentler conditions than can other preparations of the azo group; thus this method is applicable for the generation of various types of azo-conjugated metalladithiolenes that contain functional groups.

These precursors could derive corresponding metalladithiolenes by cleavage of the protecting group with phenyllithium or potassium hydroxide (Scheme 2), followed by the addition of metal halides.

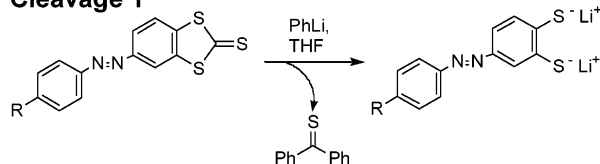
The one-pot preparation used here provided two advantages: the first was selectivity of the reaction conditions due to the choice between two different types of cleavage, and the second was a preparation of the metalladithiolene without isolation of air-sensitive dithiolate or dithiol compounds. The cleavage with phenyllithium yielded dithiolate in dry THF accompanying the loss of diphenylthioetone (Scheme 2, cleavage 1). Because some metalladithiolenes and metal halides are unstable in protic solvent, reaction in aprotic solvent is often required for metalladithiolene synthesis. In contrast, many metal halides and some dithiolate dianions are water-soluble or methanol-soluble,

(16) (a) Heck, R. F. *Inorg. Chem.* **1968**, *7*, 1513. (b) Cocker, T. M.; Bachman, R. E. *Inorg. Chem.* **2001**, *40*, 1550. (c) Xi, R.; Abe, M.; Suzuki, T.; Nishioka, T.; Isobe, K. *J. Organomet. Chem.* **1997**, *549*, 117.

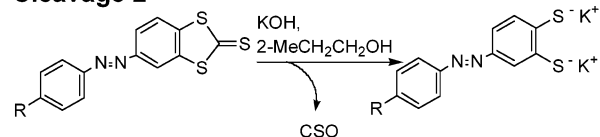
(17) Kuster, W.; Mayo, P. *J. Am. Chem. Soc.* **1974**, *96*, 3502.

Scheme 2. Cleavages of the Protecting Group

Cleavage 1



Cleavage 2



whereas they are insoluble in most organic solvents. Cleavage with potassium hydroxide in alcohol proved suitable for using such compounds as reaction reagents (Scheme 2, cleavage 2). By employing both methods, we successfully prepared various types of dithiolenes as **9–18**.

Reaction of dppeNiCl₂ and dithiolate derived from **5** by cleavage 1 gave a mixture containing air-stable Ni dithiolene **12** (Scheme 1C). **12** could be purified by silica gel column chromatography and recrystallization from CH₂Cl₂/hexane to yield orange crystals. Substituting dppePdCl₂ or dppePtCl₂ for the Ni complex in this reaction provided the corresponding metalladithiolenes, **13** and **14**, in the same manner. Low yields of these complexes, 5–13% from **5**, appear to have been the result of nucleophilic side reactions accompanying the cleavage of the protecting group by phenyllithium. Replacing the methyl group with other substituent groups had no effect on the yield of **9–11**.

Because CpCoI₂(CO) is air- and water-sensitive,^{14d} cleavage 1 was used to prepare **15** (Scheme 1C). The yield from **5** was similar to that of the dppe-metalladithiolene complexes **12–14**. On the other hand, because NiCl₂·6H₂O is soluble in water or methanol and insoluble in most organic solvents, the cleavage was carried out with potassium hydroxide (cleavage 2) to prepare **16** (Scheme 1C). The yield from **5** was similar to that of the other dithiolenes.

Reaction of **8** and phenyllithium in THF (cleavage 1) gave a slurry; the subsequent addition of dppeNiCl₂ to this slurry afforded the mononuclear complex **17** as a red solution (Scheme 1C). On the other hand, treatment of **8** with potassium hydroxide in alcohol (cleavage 2) gave a clear red solution, and the addition of dppeNiCl₂ led to a precipitation of the dinuclear complex **18** (Scheme 1C). This result can be attributed to the solubility of the dithiolate anion. In cleavage 1, the cleavage of the two protecting groups of **8** most likely proceeded stepwise, and the initially produced dianion was immediately precipitated because the charged dianion compound was insoluble in THF. Addition of dppeNiCl₂ for the complexation reaction gave a clear solution of THF-soluble mononuclear complex **17**. In the case of cleavage 2, the dianion and the tetraanion derived from **8** were soluble in alcohol; accordingly, the complete cleavage of the two protecting groups was achieved. The following complexation reaction afforded the alcohol-insoluble dinuclear complex **18** as a red precipitate. It is of note that utilizing two different cleavage conditions (i.e., cleavages 1 and 2) provided for quite different structures of the complex.

X-ray Crystallographic Analysis of 12–14. Single crystals suitable for X-ray crystallographic analysis were obtained for

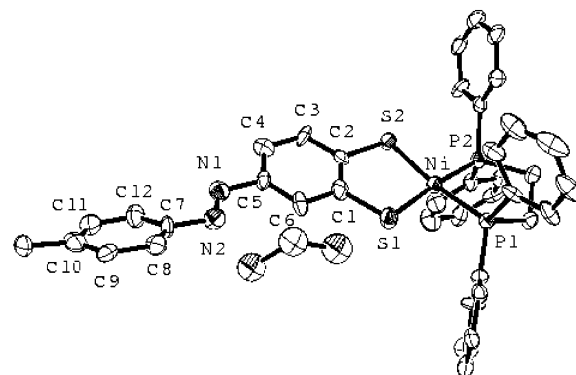


Figure 1. ORTEP plot of **12** with 50% probability of ellipsoids.

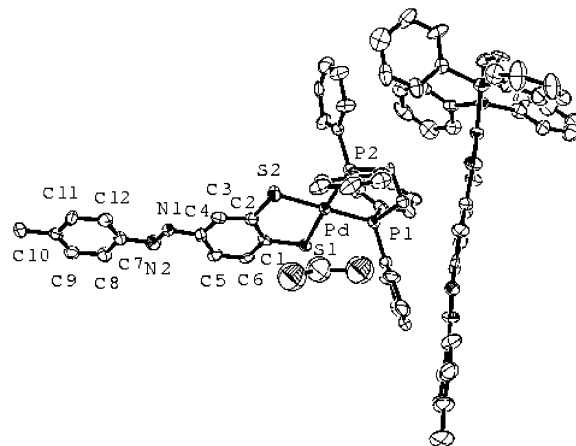


Figure 2. ORTEP plot of **13** with 50% probability of ellipsoids.

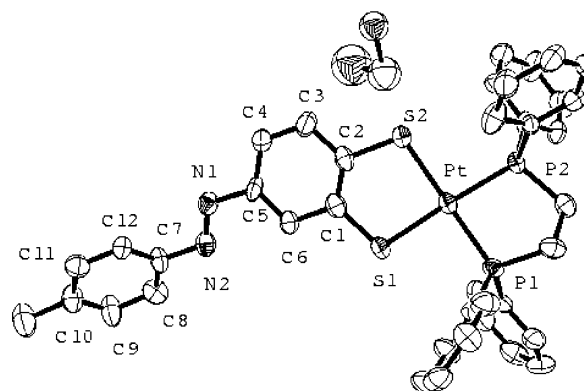


Figure 3. ORTEP plot of **14** with 50% probability of ellipsoids.

the Ni, Pd, and Pt complexes **12–14** by recrystallization from dichloromethane/hexane. ORTEP diagrams for **12–14** are displayed in Figures 1–3 (the selected bond lengths, angles, and torsion angles are summarized in Table S2, Supporting Information). In the Pd complex, **13**, there were two types of molecules having slightly different structures. The configuration around the metal center was a typical tetracoordinated square-planar structure, and a dichloromethane molecule was included as the crystal solvent. The metalladithiolene rings were planar five-membered rings, which indicated the existence of the quasi-aromaticity in these metallacycles.⁷ The bond lengths of M–S1 and M–S2 were within the usual range of M–S distances for other square-planar metalladithiolene complexes.¹⁸ In the Ni complex, **12**, the Ni–S and the S–C bonds can be best described as single bonds with lengths of 2.158(3) and 2.159(3) Å, and

Table 1. Reduction and Oxidation Potentials^a of **12–14**

complex	E^{O} or $E_{\text{p,c}}$ or $E_{\text{p,a}}/V$ vs Fc^+/Fc			
	metalladithiolene	azo	metalladithiolene	azonium ^b
12	−1.930 (rev)	−1.85	−1.98	0.31
13	−2.25 (2e [−])	−1.96	−2.08	0.38
14	−2.60 (2e [−])	−1.95	−2.22	0.45

^a E^{O} ($= (E_{\text{p,c}} + E_{\text{p,a}})/2$) values denote reversible reactions (rev. is given in parentheses), and $E_{\text{p,c}}$ and $E_{\text{p,a}}$ values are given for irreversible reduction and oxidation. The reduction is a 1e[−] process unless 2e[−] is specified in the parentheses. ^b Potentials of a new reduction wave upon the addition of acid.

1.775(9) and 1.750(9) Å, respectively, and the C1–C2 bond at 1.368(12) Å is best described as a double bond. The Pd and Pt complexes **13** and **14** had structural features in the metalladithiolene moiety similar to that of the Ni complex, **12**. Regular organic azobenzenes have a planar structure in the trans form, and the azo double bond length lies in the range of 1.23–1.27 Å.¹⁹ The configurations of the azobenzene moiety in **12–14** were all trans, but the planarity and the N1–N2 bond length of the azobenzene moiety were significantly different from each other in a comparison of complexes. In the Ni complex, **12**, the five-membered metalladithiolene ring was coplanar with a fused phenyl ring and an azo double bond; however, the planarity between the tolyl and the azo moieties was lost with a N1–N2–C7–C8 torsion angle of −158.5(11)°. On the other hand, the Pd complex **13** had an almost planar azobenzene structure that was coplanar with the metalladithiolene ring. The Pt complex, **14**, contained a significantly distorted azobenzene moiety, as can be seen in the C12–C7–C5–C4 torsion angle of 55.3°. The N1–N2 bond length in **12** and that in **13** were 1.252(9) and 1.26(2) Å, respectively, values which lie in the normal range of 1.23–1.27 Å for organic azobenzenes. The Pt complex, **14**, includes a significantly long N1–N2 double bond with a length of 1.32(2) Å. This value is closer to the single bond length of charge-distributed triazene (−N[−]–N⁺=N[−]),²⁰ rather than to that of a typical double bond. The unusual bond length indicated the existence of strong conjugation between the metalladithiolene and the azobenzene moieties.

Electrochemistry of 12–14. Cyclic voltammetry of **12–14** was carried out at a glassy carbon electrode in Bu₄NClO₄–acetonitrile (Figure S1, Supporting Information), and the results are summarized in Table 1. The complexes **12–14** show a reduction wave ascribable to the metalladithiolene moiety, in addition to irreversible two-step 1e[−] reduction waves of the azo moiety from −1.8 to −2.0 V versus Fc⁺/Fc, respectively. The Ni complex, **12**, shows a reversible wave at −1.9 V, which can be attributed to a Ni(II)/Ni(I) 1e[−] reduction.^{20a} Compounds **13** and **14** underwent an irreversible one-step 2e[−] reduction on the metal center at −2.2 and −2.6 V, respectively. The potential and reversibility of the reduction of the metalladithiolene moieties were similar to those of the related complexes,²¹ and the reduction potential was found to be more negative, that is, in the order of **14** > **13** > **12**. The reduction potentials of the

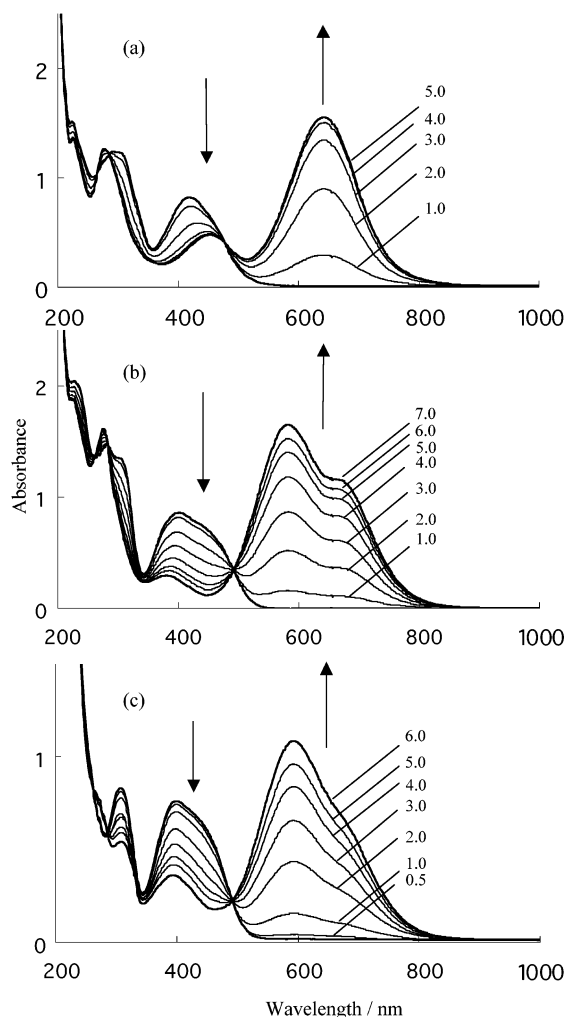
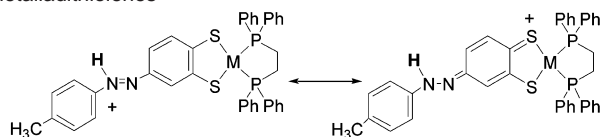


Figure 4. UV-vis spectral changes of **12** (a), **13** (b), and **14** (c) upon addition of CF₃SO₂H in MeCN. The numbers in the figure refer to the mole equivalents of the acid to the complex.

azo moiety in **12–14** were more negative than that of azotoluene (−1.70 V vs Fc⁺/Fc), and this potential shift can be attributed to the strong electron donation from the metalladithiolene moiety. The donation effect was more efficient, that is, in the order of **14** > **13** > **12**. In the oxidation of the metalladithiolene moiety, all complexes revealed a one-step irreversible wave at 0.3–0.5 V versus Fc⁺/Fc, and the order of these potentials was identical to that of the reduction potential. The results of these electrochemical measurements indicated that the π electron delocalization and the π donation ability of the metalladithiolene moiety were both the most significant in the Pt complex, **14**.

Proton Response of 9–14. Compounds **12–14** exhibited an unusual proton response together with a drastic change in color, for example, from yellow to deep green in the Ni complex, **12**, and to deep blue in the Pd and Pt complexes, **13** and **14**. Figure 4 shows the spectral changes in **12–14** upon addition of trifluoromethanesulfonic acid in MeCN. With increases in the amount of acid, the π–π* transition band of the azo moiety decreased in intensity, and a new strong band appeared in the visible region. Reverse spectral changes were achieved with the addition of potassium *tert*-butoxide. This spectral behavior was similar to that of the *N*-heterocycle-substituted metalladithiolenes,^{11e,15b,22} thus indicating that protonation of the azo moiety had taken place (Scheme 3). To examine the proton response

- (18) (a) Darkwa, J. *Inorg. Chim. Acta* **1997**, *257*, 137. (b) Landis, K. G.; Hunter, A. D.; Wagner, T. R.; Curtin, L. S.; Filler, F. L.; Jansen-Varunum, S. A. *Inorg. Chim. Acta* **1998**, *282*, 155.
 (19) (a) Işık, Ş.; Öztürk, S.; Fun, H. K.; Agar, E.; Şaşmaz, S. *Acta Crystallogr., Sect. C* **2000**, *95*. (b) Handrosch, C.; Dinnebier, R.; Bondarenko, G.; Bothe, E.; Heinemann, F.; Kisch, H. *Eur. J. Inorg. Chem.* **1999**, 1259.
 (20) (a) Boyd, G. V.; Norris, T.; Lindley, P. F.; Mahmoud, M. M. *J. Chem. Soc., Perkin Trans. 1* **1977**, 1612. (b) Boyd, G. V.; Norris, T.; Lindley, P. F. *J. Chem. Soc., Perkin Trans. 1* **1977**, 965.
 (21) (a) Bowmaker, G. A.; Boyd, P. D. W.; Campbell, G. K. *Inorg. Chem.* **1982**, *21*, 2403. (b) Bond, A. M.; Tedesco, V. *Inorg. Chem.* **1994**, *33*, 5761.

Scheme 3. Resonance Structures of Protonated Metalladithiolenes**Table 2.** λ_{\max} of Trans and Protonated Forms of **9–12** and Rate Constants^a of Cis-to-Trans Thermal Isomerization of **9–12** in MeCN

complex	trans-M		10^4 k/s^{-1}
	λ_{\max}/nm (10^{-4} $\epsilon/M^{-1} cm^{-1}$)	M-H ⁺ λ_{\max}/nm	
9	422 (1.92)	641	0.63
10	430 (2.02)	653	1.2
11	421 (2.22)	656	2.8
12	418 (1.82)	642	1.2

^a Rate constants were estimated from the first-order plots of absorption change at 35 °C.

further, electrochemical measurements were carried out upon addition of acid to **12–14**. The results are given in Table 1 (cyclic voltammograms are displayed in Figure S2, Supporting Information). Upon the addition of acid, the reduction wave of the azo moiety disappeared, and a new reduction wave was observed at a more positive potential (−0.22 to −0.28 V vs Fc⁺/Fc). This finding clearly demonstrates that the protonation of the azo moiety induces a significantly positive shift of the azo reduction potential. The reduction potentials of the protonated azo moiety were in the following order: **14** > **13** > **12**, indicating the order of stability of the protonated azo moiety. It can be deduced from these results that the protonated azo moiety is stabilized by the π electron donation from the dithiolenes ring, which is the most efficient in the Pt complex, **14**. The single protonation is supported by the results of the ESI-mass spectroscopic measurement, which show a peak at m/z 715.1 in **12**, m/z 763.1 in **13**, and 852.3 in **14**, and an isotope pattern of M-H⁺ (M = **12–14**), respectively. The protonation to the nitrogen atom bound to the tolyl moiety reasonably afforded the conjugated structure that delocalized the charge beyond the metalladithiolenes moiety (Scheme 3). The metalladithiolenes moiety, which was strongly conjugated with the azo group, increased the basicity of the azo group with a resonance stabilization effect, which in turn led to the observed facilitated protonation behavior. A strong visible band was assigned to the metalladithiolenes $\pi \rightarrow$ azo group π^* charge-transfer transition. Appearance of this band was caused by the protonation to the azo group, because the protonation, accompanying the strong conjugation with an alternative bond structure, decreased the energy gap between the metalladithiolenes moiety and the azo moiety. The wavelengths of this charge-transfer band in azo-conjugated Ni dithiolenes with various substituent groups, R (R = H, **9**; R = Cl, **10**; R = OMe, **11**; R = CH₃, **12**), are summarized in Table 2, which shows that no significant difference can be seen among the various substituted dithiolenes. This result indicates that the wavelength of this band was dominated by the electronic structure of the metalladithiolenes moiety and was furthermore independent of the substituent group on the phenyl ring.

(22) Kaiwer, S. P.; Vodacek, A.; Blough, N. V.; Pilato, R. S. *J. Am. Chem. Soc.* **1997**, *119*, 9211.

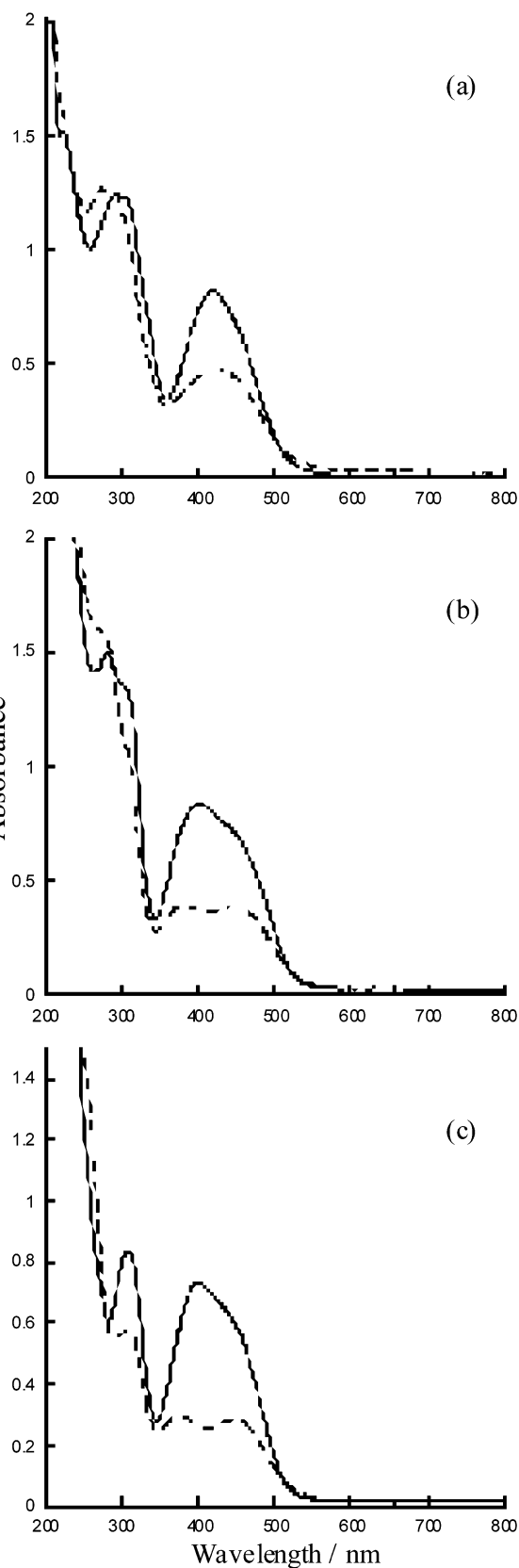


Figure 5. UV-vis spectra of **12** (a), **13** (b), and **14** (c) in MeCN before (solid line) and after (dotted line) photoirradiation by UV light at 405 nm.

Photo Response of 12–14. Figure 5 shows UV-vis absorption spectra of **12–14** in MeCN before and after photoirradiation with a UV light at 405 nm. A $\pi-\pi^*$ transition band ascribable

to the azo moiety in the trans form can be observed at 405 nm ($18\,200\text{ M}^{-1}\text{ cm}^{-1}$), 405 nm ($22\,300\text{ M}^{-1}\text{ cm}^{-1}$), and 405 nm ($23\,700\text{ M}^{-1}\text{ cm}^{-1}$) for **12–14**, respectively, because the $\text{M}(\text{S}_2\text{C}_6\text{H}_4)(\text{dppe})$ ($\text{M} = \text{Ni, Pd, Pt}$) does not give a strong band in this region. The bands are significantly shifted to a lower energy for **12–14**, as compared with those of regular azobenzene derivatives,¹ an effect which was due to strong conjugation and high delocalization between the metalladithiolenes and the azo moiety. In regular organic azobenzenes, a nearly linear correlation exists between the lower energy shift of the $\pi-\pi^*$ transition band and the stability of the cis form,²³ and thus some of these compounds with a lower shifted $\pi-\pi^*$ transition band may have shown no efficient photo response.^{1a} Despite the large low-energy shift of the $\pi-\pi^*$ transition, **12–14** showed a distinguishable reversible photo response. The $\pi-\pi^*$ transition band decreased in intensity after photoirradiation, indicating the occurrence of trans-to-cis photoisomerization. The cis-to-trans reverse reaction occurred, allowing perfect recovery of the spectra of the trans forms, in response to photoirradiation at 360 nm in **12**, and at 310 nm in **13** and **14**, respectively. The reversible isomerization reaction was also observed by a ^1H NMR spectroscopic measurement. The integration ratio of the signals for trans and cis forms indicated that ca. 40% of the trans form was converted to the cis form by photoirradiation at 405 nm in a photostationary state. Although the transition corresponding to these UV light energies has not been specified, it is intriguing that the cis-to-trans isomerization is promoted by UV light with an energy higher than the $\pi-\pi^*$ transition, because the regular azobenzenes undergo isomerization by irradiating the $n-\pi^*$ band in the visible region.^{1b}

Thermal Isomerization of 9–12. Organic azobenzenes have been known to show cis-to-trans thermal isomerization, the rate of which is strongly affected by *para*-substituent groups.²³ Referring to the ability of the electron donor and acceptor substituted on the two phenyl groups, Rau^{1a} classified the azobenzenes into three groups: (i) the azobenzene type, (ii) the aminoazobenzene type, and (iii) the pseudo-stilbene type. In the case of (i), that is, azobenzene without donor or acceptor substituents, an absorption peak corresponding to the $\pi-\pi^*$ transition appeared around 350 nm, and thermal isomerization was very slow (more than 1 day at ambient temperature). For type (ii) with the donor group on the *para*-position of the phenyl ring, an absorption peak assigned to the $\pi-\pi^*$ transition appeared at ca. 400 nm, which was longer than the wavelength of type (i). The thermal isomerization was also faster in the case of the type (ii) compounds (several hours). The last type (iii), with donor and acceptor substituents on the *para*-position of each phenyl group (the so-called push-pull type), exhibited a maximum absorption peak attributed to the $\pi-\pi^*$ transition in the visible region (longer than 400 nm). The thermal isomerization of type (iii) was much faster (several minutes or seconds) than that of type (ii) and strongly depended on the polarity of the environment. In this study, cis-to-trans isomerization was investigated for azo-conjugated Ni dithiolenes with various substituent groups, R ($\text{R} = \text{H}$, **9**; $\text{R} = \text{Cl}$, **10**; $\text{R} = \text{OMe}$, **11**; and $\text{R} = \text{CH}_3$, **12**). The estimated first-order rate constants for cis-to-trans isomerization for **9–12** at 35 °C and the λ_{max} of

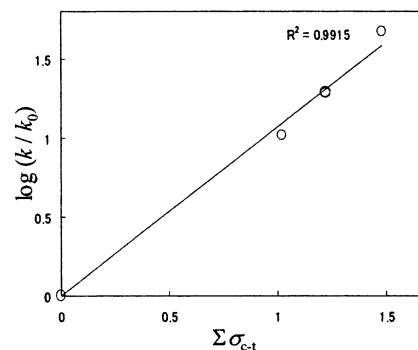


Figure 6. Correlation between $\Sigma\sigma_{c-t}$ and $\log(k/k_0)$.

these complexes are listed in Table 2. The wavelengths of absorptions in these complexes were almost identical to each other and were independent of the substituent group. In contrast, the rate constants of the cis-to-trans isomerization were strongly dependent on the substituent group. Nishimura et al.²³ reported that the introduction of substituents almost invariably accelerated the rate, irrespective of the nature of the substituents. The substituent effect was of an additive nature, and the following Hammett-type equation holds approximately, as

$$\log k/k_0 = \sum \sigma_{c-t} \quad (2)$$

where k_0 and k refer to the rate constant of an azobenzene²⁴ and of substituted azobenzene derivatives, and σ_{c-t} denotes a substituent constant characteristic of the type and the position of the substituent in question. Using this equation and the rate constant for the nonsubstituted Ni dithiolenes complex, **9**, we estimated the substituent constant for Ni dithiolenes as $\sigma_{c-t} = 1.02$. Using this value and the known substituent constant (CH_3 ; $\sigma_{c-t} = 0.22$, Cl; $\sigma_{c-t} = 0.22$, OMe; $\sigma_{c-t} = 0.46$), we plotted $\log k/k_0$ values against σ_{c-t} for **9–12** according to eq 2 (Figure 6). A positive correlation was found to exist between $\log k/k_0$ and σ_{c-t} , which indicated that metalladithiolenes also obey the additive rule for the cis-to-trans isomerization rate constant of organic azobenzenes and that the stability of the cis form for substituted azo-conjugated metalladithiolenes can thus be predictable. Furthermore, although metalladithiolenes exhibit the $\pi-\pi^*$ transition band shifted to a lower energy, the stability of the cis form was higher than that of such organic azobenzenes. It can be considered that tactics to induce a lower-shifted $\pi-\pi^*$ transition band in organic azobenzenes are most likely limited, and the donor-acceptor substituent groups are introduced for most of the compounds²⁵ (i.e., type (iii)), for which the rate of rotational isomerization is much accelerated. Consequently, azo-conjugated Ni dithiolenes **9–12** can be classified as type (ii) or type (iii) in the absorption peak of the $\pi-\pi^*$ transition, as well as type (i) in regards to the stability of the cis form. The results described above indicate that the use of azo-conjugated metalladithiolenes offers an efficient method of lowering the transient energy needed for isomerization, while maintaining the stability of the cis form.

(24) Talaty, E. R.; Fargo, J. C. *J. Chem. Soc., Chem. Commun.* **1967**, 65.

(25) (a) King, N. R.; Whale, E. A.; Davis, F. J.; Gilbert, A.; Mitchell, G. R. *J. Mater. Chem.* **1997**, 7, 625. (b) Charlton, M. H.; Docherty, R.; Mcgeein, D. J.; Morley, J. O. *J. Chem. Soc., Faraday Trans.* **1993**, 89, 1671. (c) Wildes, P. D.; Pacifici, J. G.; Irick, G., Jr.; Whitten, D. G. *J. Am. Chem. Soc.* **1971**, 93, 2004.

(23) (a) Nishimura, N.; Kosako, S.; Sueishi, Y. *Bull. Chem. Soc. Jpn.* **1984**, 57, 1617. (b) Nishimura, N.; Sueyoshi, T.; Yamanaka, H.; Imai, E.; Yamamoto, S.; Hasegawa, S. *Bull. Chem. Soc. Jpn.* **1976**, 49, 1381. (c) Sueyoshi, T.; Nishimura, N.; Yamamoto, S.; Hasegawa, S. *Chem. Lett.* **1974**, 1131.

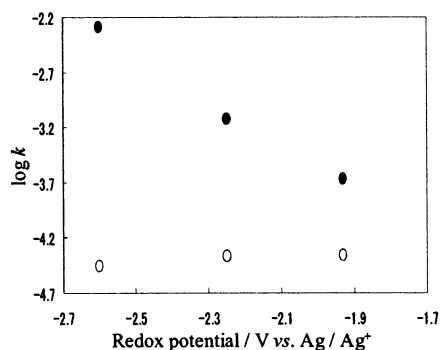


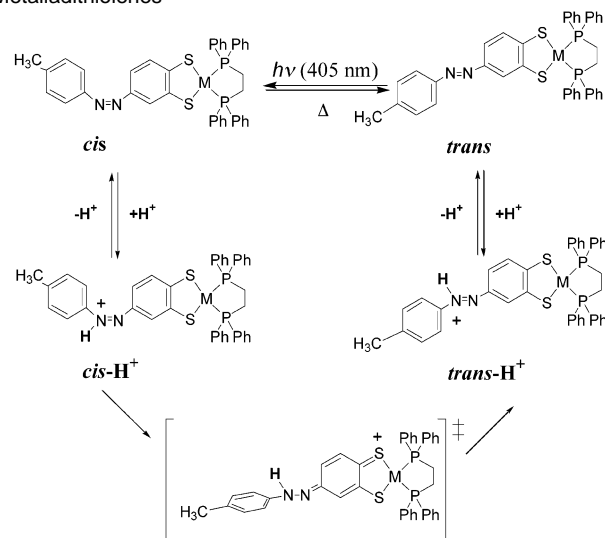
Figure 7. Correlation between redox potentials and rate constant k (white) and k_{acid} (black) for **12–14**.

Proton-Catalyzed Cis-to-Trans Isomerization of **12–14**.

The proton response of the cis form was then investigated. When a slight amount of acid was added to a solution containing cis-**12–14** prepared by photoirradiation, immediate cis-to-trans transformations were observed. The rate constants of cis-to-trans thermal and proton-catalyzed isomerization upon addition of 0.01 equiv of $\text{CF}_3\text{SO}_3\text{H}$ for **12–14** at 23.3 °C are displayed in correlation with the reduction potentials of nonprotonated forms in Figure 7. The rate constant of thermal isomerization, k (s^{-1}), was independent of the differences among the central metals, whereas the rate constant of proton-catalyzed isomerization, k_{acid} (s^{-1}), strongly depended on the metal center. The k_{acid} reaches $5.1 \times 10^{-3} \text{ s}^{-1}$, which is 150 times larger than k , in the Pt complex **14**, whereas the significant acceleration by addition of the acid in the same condition was not observed for azobenzene ($k = 2 \times 10^{-6} \text{ s}^{-1}$, $k_{\text{acid}} = 3 \times 10^{-6} \text{ s}^{-1}$). A positive correlation existed between the rate constant, k_{acid} , and the reduction potential of the metalladithiolenes. This result indicated that the rate constants of the proton-catalyzed isomerization were exponentially proportional to the redox potentials of the metalladithiolenes and that the acceleration was efficient by shifting the reduction potential in the negative direction. It can be deduced that the reduction potential of the metal center is closely related to the electron-withdrawing ability of the metal center, which accompanies the electron-donation ability of the dithiolene ring. In the case of the Pt complex **14**, the reduction potential of which was more negative than that of **12** and **13**, strong donation to the azo group was exhibited; such donation stabilized the transient state with the resonance effects. Accordingly, the acceleration of isomerization was closely related to the reduction potential of the metal center.

The proton-assisted phenomenon indicated that a protonated cis form, cis- H^+ , instantly produced the trans form, trans- H^+ , followed by the formation of the trans form accompanying deprotonation (Scheme 4). In this isomerization, it can be presumed that the transient structure was the charge-distributed structure (Scheme 4), in which the protonated nitrogen atom changed its hybridization from sp^2 to sp^3 . This activated species, with substantial single-bond character in the azo group, was stabilized by the strong conjugation between metalladithiolene and the azo moiety, and thus the rotational barrier for the cis-to-trans isomerization was expected to be much smaller than that expected for the thermal isomerization. The reduced activated energy caused acceleration in the rate of the cis-to-trans isomerization. In conclusion, azo-conjugated metalladithiolenes exhibited a novel isomerization behavior, that is, “proton-

Scheme 4. Photo and Proton Responses of Azo-Conjugated Metalladithiolenes



catalyzed cis-to-trans isomerization”. The mechanism of the proton-catalyzed cis-to-trans isomerization can be used to predict that the π donation ability of the dithiolene ring might be considerably influential in regards to the isomerization behavior. The type of central metal was dominant to the electronic state of the dithiolene ring, and thus isomerization could be controlled in such instances by use of different metal centers.

Conclusion

A versatile synthetic method of the azo-conjugated metalladithiolene system using a dithiolate-protected nitroso compound **2** was developed. In this system, a novel proton response of the azo group occurred due to the strong electron-donating effect of the metalladithiolene moiety. This led to a novel proton-catalyzed cis-to-trans isomerization in dppe-M complexes **12–14**, and this isomerization rate correlated with the redox potential of the metalladithiolene moiety. The trans-to-cis photoisomerization of **12–14** occurred at a considerably lower energy as compared to that of azobenzene, and the thermal stability of the cis form was much higher than that of the organic azobenzene derivatives showing similar low-energy trans-to-cis photoisomerization. The results of this systematic study of various azo-conjugated metalladithiolenes suggested that a wide range of isomerization behaviors of azo-conjugated metalladithiolenes can be controlled by adjusting the chemical structure, the electronic structure, the substituent groups, and the redox potential of metalladithiolenes.

Acknowledgment. This work was supported by Grants-in-Aid for scientific research (Nos. 13022212, 14050032, and 14204066) from the Ministry of Education, Science, Sports and Culture, Japan. The authors thank Y. Namiki for his experimental assistance.

Supporting Information Available: Experimental section for synthesis and text for the photo and proton response of **15–18**, crystal parameters and X-ray diffraction data (Table S1) and selected bond lengths, angles, and torsion angles for **12**, **13**, and **14** (Table S2), cyclic voltammograms of **12–14** in the absence of protons (Figure S1) and in the presence of protons (Figure S2), cyclic voltammograms of **15** in the absence of

protons (Figure S3) and in the presence of protons (Figure S4), UV-vis spectral change by photoirradiation of **15** (Figure S5), cyclic voltammogram of **16** (Figure S6), UV-vis spectra of **16** and its reduced form (Figure S7), UV-vis spectral change in **16** by protonation (Figure S8), and UV-vis spectral change by

photoirradiation and by protonation of **17** and **18** (Figures S9 and S10, respectively) (PDF and TXT). This material is available free of charge via the Internet at <http://pubs.acs.org>.

JA028080P